Annals of Nuclear Energy 165 (2022) 108641

Contents lists available at ScienceDirect

Annals of Nuclear Energy

journal homepage: www.elsevier.com/locate/anucene

Extension of SCALE/Sampler's sensitivity analysis ☆

Friederike Bostelmann *, Dorothea Wiarda, Goran Arbanas, William A. Wieselquist

Oak Ridge National Laboratory, P.O. Box 2008, Bldg.5700, Oak Ridge, TN 37831, USA

ARTICLE INFO

Article history:
Received 22 April 2021
Received in revised form 23 July 2021
Accepted 12 August 2021

Keywords:
Sensitivity analysis
Correlation coefficient
Nuclear data
Random sampling
SCALE
Sampler

ABSTRACT

Nuclear data are a major source of uncertainties in reactor physics calculations. The propagation of nuclear data uncertainties to important system responses is instrumental when determining appropriate safety margins in reactor safety analyses. It is also important to understand the major contributors to the observed uncertainties to make recommendations for further measurements and evaluations and aid in the understanding of the studied system.

The SCALE code system allows for nuclear data uncertainty analysis based on the random sampling approach as implemented in SCALE's Sampler sequence. Sampler was recently extended by a sensitivity analysis in terms of the calculation of two correlation-based sensitivity indices. This analysis allows for the identification of the top contributing nuclear reactions to any analyzed output uncertainty. This paper presents the sensitivity indices, along with their interpretation and limitations. It demonstrates the application in an eigenvalue and decay heat analysis for a boiling water reactor fuel assembly.

1. Introduction

In nuclear safety analyses for licensing processes, there is an increasing interest in replacing conservative calculations with best-estimate calculations supplemented by uncertainty analyses. This is also known as *best estimate plus uncertainty (BEPU)* (D'Auria et al., 2012). In a best-estimate calculation, the physical processes in nuclear power plants are realistically described. Uncertainties of output parameters are then determined based on uncertainties of the input parameters to the applied computer code (Boyack et al., 1990).

For reactor physics calculations, the input uncertainties may be grouped as follows:

1. manufacturing uncertainties, including geometric dimensions and initial material compositions,
2. reactor system state, such as the evolving fuel temperature and moderator density, and
3. uncertainties of the nuclear data.

Other relevant uncertainties are associated with the methods and modeling approximations in the applied codes, as well as user errors.

Nuclear data are among the most important types of uncertain input parameters. They are subject to systematic and statistical uncertainties because they are determined through measurements and subsequent evaluations. Evaluated nuclear data files, such as the file in the Evaluated Nuclear Data File (ENDF/B) (Chadwick et al., 2011) library, provide uncertainties and corresponding correlations of nuclear data in the form of covariance matrices.

In uncertainty analyses, uncertainty data are propagated through the calculation chain to determine uncertainties of the output quantities of interest resulting from this data. Sensitivity analyses can provide information about the contribution of individual uncertain input parameters to the output uncertainty. When determining the major drivers of observed uncertainties, recommendations can be made for measurements of particular nuclear data.

1.1. Uncertainty and sensitivity analysis methods

For nuclear data uncertainty and sensitivity analysis, the two most common methods in use are (1) an approach based on perturbation theory and (2) the random sampling approach.

For the perturbation-theory approach, sensitivities of quantities of interest—such as the multiplication factor, reaction rates, and

* Corresponding author.
E-mail address: bostelmannf@ornl.gov (F. Bostelmann).

https://doi.org/10.1016/j.anucene.2021.108641
0306-4549/

reactivity coefficients—due to changes in the nuclear data are determined using perturbation theory. These sensitivities are determined for the cross sections of all nuclide reactions considered in the investigated model in all energy groups. The sensitivity of a response to a cross section in a certain energy group describes how much the response would change due to a change in this particular cross section. (Williams, 1986).

Multiplication of all sensitivity coefficients with the corresponding covariance matrices results in the uncertainty of the system response. Furthermore, when multiplying only the sensitivities of one nuclide reaction with the corresponding covariance matrix, the contribution to the output uncertainty of only the specific covariance matrix, i.e. the contribution of the uncertainties of one nuclide reaction, can be determined. This sensitivity analysis is usually a byproduct of the analysis.

In the random sampling approach, nuclear data are sampled using conditional sampling based on the covariance data. After a set of calculations has been run with the perturbed data, a statistical analysis is performed to estimate the uncertainty of the response of interest through the standard deviation or other quantities. The use of this approach in combination with a code for generation of macroscopic few-group cross sections enables straightforward full core uncertainty analysis. The coupling of a full core nodal code to a thermal hydraulics code allows for uncertainty analyses of steady-state and transient calculations.

In addition to being a simple, straightforward approach, random sampling provides two main advantages over the perturbation theory–based approach. (1) When using random sampling, any calculation's output quantity can be statistically analyzed, whereas the perturbation theory–based approaches available in current simulation software are limited to responses such as the eigenvalue, reactivity differences, and reaction rate ratios. For safety analyses in particular, flux and power distributions are needed to confirm compliance with safety limits. Currently, the only way to easily calculate corresponding uncertainties is to use the random sampling approach with current simulation software. (2) The assumption of linearity of changes in quantities of interest to input has been shown to be adequate for the calculation of quantities such as as the multiplication factor and reactivity coefficients in steady-state calculations. However, this assumption no longer holds for all points in time during a transient analysis (Aures et al., 2020). Since the random sampling approach does not make assumptions of linearity, it can be applied to any steady-state or transient analysis.

A disadvantage of the random sampling approach is the increased computation time needed to achieve a sample size that is sufficient to obtain a statistically significant result. However, with increasing availability of large computing clusters, the application of this approach has become tractable, even for complex models. Furthermore, a sensitivity analysis to identify important nuclide reactions for the output uncertainty is not a byproduct of the analysis. It is possible to perform individual sets of calculations based on perturbed cross sections of only one nuclide reaction. However, repeating this for all relevant nuclide reactions is very computationally expensive and depending on the approach might disregard the influence of correlations between different nuclide reactions. Other options include calculation of sensitivity indices based on (1) correlations determined as part of the post-processing (Bostelmann et al., 2018) or (2) an approach based on variances similar to Sobol' indices for which the calculation is again computationally expensive due to the presence of correlations between nuclear data (Sobol, 1993; Krzykacz-Hausmann, 2006).

1.2. Existing tools for uncertainty and sensitivity analysis

The SCALE code system is a widely used tool for reactor physics, criticality safety, radiation shielding, and spent fuel characterization for nuclear facilities and transportation/storage package designs. SCALE is developed at Oak Ridge National Laboratory and includes several modules for sensitivity and uncertainty analysis, covering both the perturbation theory approach in SCALE's the TSUNAMI code (Broadhead et al., 2004; Rearden et al., 2011) and the random sampling approach in SCALE's Sampler code (Williams et al., 2013).

TSUNAMI has been part of SCALE for several years, but Sampler is a relatively new development. In its current implementation, Sampler is a super sequence that applies cross section perturbations generated based on covariance data to any SCALE module that uses multi-group cross sections. The consistency between uncertainty results obtained with TSUNAMI and Sampler has been demonstrated several times before (Williams et al., 2013; Bostelmann et al., 2015a). The statistical analysis in Sampler has so far been limited to the calculation of the average and standard deviation of output quantities of interest, as well as covariances and correlations between different quantities. Recently, a sensitivity analysis was added that allows the user to identify the most relevant nuclide reactions for the investigated output uncertainty.

Sampler's new indices are based on methods developed for the XSUSA code, a cross section uncertainty analysis code developed at the Gesellschaft für Anlagen- und Reaktorsicherheit (GRS) (Bostelmann et al., 2015b). XSUSA can calculate indices based on correlations of nuclear data perturbations with the output to estimate the importance of the individual nuclide reactions for the output uncertainty (Bostelmann et al., 2018). The calculation of Sobol' main effect and total effect sensitivity indices was previously demonstrated and shown to provide almost consistent results with these correlation indices (Bostelmann, 2020). Other codes that use the random sampling approach for nuclear data uncertainty analysis are the PSI codes SHARK-X (Wieselquist et al., 2013), the Sandia National Laboratory code DAKOTA (Swiler et al., 2018) and NUSS (Zhu et al., 2015), as well as the fast Total Monte Carlo (TMC) code developed by the Nuclear Research and Consultancy Group (NRG) (Rochman et al., 2014). XSUSA, DAKOTA and SHARX-X perturb nuclear data based on covariance data provided in evaluated nuclear data files. In contrast, TMC perturbs all possible model input parameters (e.g., level densities and optical models) of a nuclear reaction code based on the physical theoretical background. SHARK-X includes a method to calculate sensitivity coefficients using a least squares solver that can be multiplied with covariance matrices to obtain uncertainty contributions (Hursin et al., 2016). DAKOTA can calculate several correlation coefficients (Adams et al., 2020). NUSS includes a global sensitivity analysis with variance decomposition to rank reactions in terms of their variance contributions (similar to Sobol' indices) (Zhu et al., 2016). With TMC, sensitivities can be obtained through direct perturbations of input parameters (Rochman et al., 2011).

1.3. Scope of this paper

This paper presents the theoretical background of Sampler's new sensitivity indices, as well as the interpretation considering all relevant details. Application of the sensitivity indices is demonstrated through the depletion and decay analysis of a boiling water reactor (BWR) assembly. Required conditions and limitations for the calculation, and potential challenges in the practical application are discussed. The flexibility in Sampler's uncertainty analysis to investigate any output quantity of interest is demonstrated through the examination of not only the eigenvalue during depletion, but also the development of the decay heat subsequent to irradiation which cannot be studied using common perturbation theory-based approaches.

The results presented in this paper were generated with a prerelease of SCALE 6.3.

2. Sensitivity analysis methods

While top contributing nuclide reactions to the output uncertainty are identified as a side product when using perturbation theory, it is challenging to conduct a similar study for the random sampling approach because the reliability of sensitivity results depends on the number of uncertain input parameters and the sample size. Because the analysis using linear perturbation theory is limited to a certain number of output responses, it is nevertheless desirable to use the random sampling approach to identify important nuclide reactions that contribute to the uncertainty of additional safety-relevant output quantities such as peak power, decay heat, or various reactivity coefficients.

One method for determining the contribution of individual cross sections to the output uncertainty in random sampling calculations involves one-at-a-time calculations. If the cross sections of one nuclide reaction are perturbed and calculations are performed based on only these perturbations, then the statistical analysis results in the output uncertainty are caused only by this nuclide reaction. However, this approach requires an additional set of calculations for each nuclide reaction, and it also does not account for correlations between different nuclide reactions. Ideally, the calculation of importance indicators should account for correlations and should be computationally inexpensive.

Based on developments performed at GRS for the XSUSA code (Bostelmann et al., 2015b), the sensitivity analysis for nuclear data perturbation calculations of the random sampling code Sampler in the SCALE code system is extended by the squared multiple correlation coefficient R^2 and the semi-partial multiple squared correlation coefficient SPC^2. R^2 and SPC^2 provide two complementary methods for determining the uncertainties' contribution of a nuclide reaction to the output uncertainty.

This section provides the mathematical description and interpretation of sensitivity indices as importance indicators to identify the most significant nuclide reactions for output uncertainties. The first part describes the variance-based sensitivity indices—the so-called Sobol' main effect and total effect sensitivity indices—and based on this description, the sensitivity indices R^2 and SPC^2 for the random sampling approach are presented.

The following descriptions are generally valid for any set of input parameters and for any output quantity of any code for which the determination of sensitivity indices is desired as part of the output analysis. For nuclear data uncertainties, the following denotations are used:

- Input parameters are the nuclear cross sections of nuclide reactions in a particular energy-group structure. That is, each cross section of a particular energy group indicated with Σ is an individual parameter.
- A parameter group includes all cross sections of an individual nuclide reaction. For example, if the ^{235}U fission cross section is provided in 56 energy groups, the fission cross sections in these 56 groups (56 individual parameters) form one parameter group.
- A model's relevant cross sections are divided into two groups: group A includes the group of cross sections of interest (Σ_A), usually all the cross sections of a particular reaction of a nuclide, and group B includes all other cross sections of the model (Σ_B).
- The number of parameters in a group are indicated with k. The maximum number of k is the number of energy groups in a covariance library.
- The output quantity of interest is indicated with Y.
- The sample size in case of the random sampling approach is indicated with N.

Given that the maximum number of independent parameters k in a group is the number of energy groups in a covariance library, k is designated as 56 and 252 in the examples provided in this section to match the number of energy groups in the covariance libraries provided with SCALE.

2.1. Variance-based sensitivity indices

Variance-based sensitivity analysis, sometimes referred to as the Sobol' method (in the case of independent parameters), is used to determine the influence of individual input parameters or groups of parameters on the variance of the model output (Sobol, 1993; Saltelli et al., 2008; Saltelli et al., 2010). The general method of this variance-based approach is described in the following.

Given the model $Y = f(\Sigma_A, \Sigma_B)$—where Y is the scalar output quantity of interest, A is the group of input parameters under consideration, and B is the complementary (residual) group—the reductive effect variance-based sensitivity index (first-order sensitivity index, or **S**obol's **M**ain effect sensitivity index in case of independent parameters), is defined as follows:

$$SM_A = \frac{Var(\mathrm{E}[Y|\Sigma_A])}{Var(Y)} = \frac{Var(Y) - \mathrm{E}[Var(Y|\Sigma_A)]}{Var(Y)} = 1 - \frac{\mathrm{E}[Var(Y|\Sigma_A)]}{Var(Y)}. \quad (1)$$

SM_A is the relative variance of the conditional expectation of Y given A: that is, the best approximation of Y in the parameters of group A. It also reveals the variance reduction of Y that is expected if the true values of parameter group A were to become known. This factor consequently indicates for which group of input parameters the reduction of uncertainties would lead to a significant reduction of the total output uncertainty. In the case of nuclear data uncertainties, SM_A can point out the nuclide reaction for which reduced cross section uncertainties would lead to significantly improved results based on more accurate measurements.

The incremental sensitivity index (**S**obol's **T**otal effect sensitivity index in case of independent parameters) can be expressed as follows:

$$ST_A = \frac{\mathrm{E}[Var(Y|\Sigma_B)]}{Var(Y)} \overset{(Eq.\ 1)}{=} 1 - SM_B. \quad (2)$$

ST_A reveals the remaining variance that is expected if the true values of the complementary group B were to become known.

Krzykacz-Hausmann (Krzykacz-Hausmann, 2006) showed that the expression for SM_A in Eq. (1) is equal to the sample Pearson correlation coefficient r between the output Y and the conditional expectation $\mathrm{E}[Y|\Sigma_A]$:

$$SM_A = \frac{Var(\mathrm{E}[Y|\Sigma_A])}{Var(Y)} = r(Y, \mathrm{E}[Y|\Sigma_A]). \quad (3)$$

For the practical application, this means that the correlation between the output of two sets of calculations is calculated as follows:

1. The first reference set of calculations is based on the standard randomly sampled input parameters.
2. The second set of calculations is based on input parameters generated as follows: the sampled parameters of group A are identical to the reference set, and a new set of new randomly sampled parameters is generated only for group B based on (i.e., under the condition of) the known perturbations of groups A.

See (Bostelmann, 2020) for details on standard and conditional sampling.

Accordingly, the incremental sensitivity index is calculated based on the correlation of the reference set of calculations and a second set using newly generated perturbations for group A while keeping the perturbations of group B from the reference set:

$$ST_A = 1 - SM_B = 1 - r(Y, \mathrm{E}[Y|\Sigma_B]). \tag{4}$$

With a sample size N, the sample correlation coefficient between two quantities a and b is determined from the covariance and the standard deviations σ:

$$r(A,B) = \frac{Cov(A,B)}{\sigma_A \sigma_B} = \frac{\sum_{i=1}^{N}(a_i - \bar{a})(b_i - \bar{b})}{\sqrt{\sum_{i=1}^{N}(a_i - \bar{a})^2}\sqrt{\sum_{i=1}^{N}(b_i - \bar{b})^2}}, \tag{5}$$

where $\bar{a}$ and $\bar{b}$ are the mean values of a and b, respectively.

While the determination of SM_A and ST_A seems to be a straightforward calculation, it requires a significant computational effort because additional sampling calculations are required for each parameter group of interest. For example, when using a sample size of 1,000 and assuming 6 reactions per nuclide, a problem with only 10 nuclides requires $(6 \cdot 10 + 1) \cdot 1{,}000 = 61{,}000$ individual calculations (nominal calculation plus one additional calculation per nuclide reaction of interest) to determine either SM_A or ST_A for all nuclide reactions. For the purpose of a simple determination of a sensitivity index based on only a single set of sampling calculations, i.e. at a much smaller computational cost, it is more practical to use linearized versions of SM_A and SM_B, respectively, as explained in the following section.

2.2. Correlation-based sensitivity indices using randomly sampled input parameters

This section includes the explanation of linearized versions of the variance-based sensitivity indices SM_A and SM_B.

2.2.1. R^2 – squared multiple correlation coefficient

A linearized version of the reductive effect sensitivity index SM_A is found in the *squared multiple correlation coefficient* R^2 (derivation shown in Appendix A). This coefficient is determined from correlations of the calculated output quantity Y with the sampled input parameters Σ_A of group A while accounting for correlations between the input parameters (Glaeser, 2008; Glaeser, 2012):

$$R^2_{Y,A} = \boldsymbol{r}_{Y,A} \mathbf{C}^{-1}_{AA} \boldsymbol{r}^t_{Y,A}, \tag{6}$$

with vector $\boldsymbol{r}_{Y,A}$ of size k containing the sample correlation coefficients r_N (calculated from sample size N) between the output Y and the input parameters of group A:

$$\boldsymbol{r}_{Y,A} = (r_N(Y,\Sigma_1), \ldots, r_N(Y,\Sigma_k)), \tag{7}$$

and matrix $\mathbf{C}_{AA}$ of size $(k \times k)$ containing the sample correlation coefficients between the input parameters:

$$\mathbf{C}_{AA} = \begin{pmatrix} r_N(\Sigma_1,\Sigma_1) & r_N(\Sigma_1,\Sigma_2) & \cdots & r_N(\Sigma_1,\Sigma_k) \\ r_N(\Sigma_2,\Sigma_1) & r_N(\Sigma_2,\Sigma_2) & \cdots & r_N(\Sigma_2,\Sigma_k) \\ \vdots & \vdots & \ddots & \vdots \\ r_N(\Sigma_k,\Sigma_1) & r_N(\Sigma_k,\Sigma_2) & \cdots & r_N(\Sigma_k,\Sigma_k) \end{pmatrix}. \tag{8}$$

It is important to stress that here the correlation matrix used in the calculation of R^2 is not the population correlation matrix that was initially used for the random sampling. Rather, it is the matrix containing the sample correlation coefficients between the sampled input parameters. If the sample size approaches infinity, then the sample correlation matrix of group A converges toward the correlation matrix that is used for sampling of group A.

Analogous to the interpretation of SM_A, R^2 can be interpreted as the expected amount by which the total output variance would be reduced if the true values of the input parameter group A become known (Glaeser, 2008). In other words, R^2 is the fraction of the output variance caused by the uncertainties of parameter group A, including the fraction of uncertainties that it has in common with other parameter groups due to correlations (Glaeser, 2012). Using a linearized method may seem contradictory with the benefit of the random sampling approach to consider nonlinear effects. However, the uncertainties are still calculated assuming any true nonlinear effects, so it is simply a linear model used to decompose the variance among all possible sources.

R^2 has the following characteristics:

- $0 < R^2_{Y,A} < 1$, with the above given interpretation,
- $R^2_{Y,A} = 0$ if zero variance in Y is explained by linear relationships with group A,
- $R^2_{Y,A} = 1$ if all variance in Y is explained by a linear relationships with group A, and
- $R^2_{Y,A} = \boldsymbol{r}_{Y,A} \cdot \boldsymbol{r}_{Y,A} = r^2_{Y,\Sigma_1} + r^2_{Y,\Sigma_2} + \ldots$ if the parameter group A contains completely uncorrelated data.

R^2 can be determined from the results of a single set of calculations for any group of parameters. The only condition for determining this coefficient is that the sample size N must be larger than the number of parameters k in the group of interest; if the sample size is smaller than k, then matrix $\mathbf{C}_{AA}$ is not positive definite, and consequently, it cannot be inverted. For the same reason, input parameters within a group must not have a total linear correlation. This problem is avoided by only considering the independently sampled input parameters in the analysis.

Total R^2

From the theoretical standpoint, the selection of parameters within a group only from a certain nuclide reaction is arbitrary. It is possible to select any set of individual parameters for the calculation of R^2. A special case is the consideration of all parameters of a model. With this analysis, it is possible to investigate the system for effects of non-linearity.

If parameter group A includes all the input parameters of the model under investigation, then the total correlation coefficient R^2_{tot} can be determined. If nonlinear effects are insignificant, then

$$Var(Lin[Y|\Sigma]) = Var(Y) \Rightarrow R^2 = R^2_{Y,A+B} = R^2_{tot} = 1. \tag{9}$$

Conversely, the calculation of R^2_{tot} allows for the assessment to determine whether nonlinear effects are negligible: if R^2_{tot} shows a significant deviation from 1 when all input parameters are considered, then it can be concluded that the output uncertainty is significantly influenced by nonlinear effects.

Adjusted R^2

It is important to note that R^2_{tot} approaches 1 if the sample size N is close to the number of sampled input parameters k in the model. This is because R^2_{tot} corresponds to the coefficient of determination for regression analysis that is dependent on the difference between N and k, the degrees of freedom in a problem. If $N - k$ is getting smaller, then R^2_{tot} converges to 1 because, in this case, it is fitted to all or almost all the degrees of freedom in this regression analysis.

To consider the dependence on the degrees of freedom, the coefficient of determination can be adjusted (Golberg and Cho, 2004):

$$\overline{R}^2 = 1 - \left(1 - R^2\right)\frac{N-1}{N-k-1}. \tag{10}$$

Since $\frac{N-1}{N-k-1} > 1$, it can be shown that $\overline{R}^2 < R^2$. This means that R^2 is overestimated, and the adjustment leads to a slight reduction.

Fig. 1 presents the bias $R^2 - \overline{R}^2$ as a function of R^2 for various sample sizes. The sample sizes are chosen as multiples of k ($N = x \cdot k$) to demonstrate the magnitude of adjustment depending on the degrees of freedom. When considering all relevant parameters for determining R^2_{tot} such that R^2_{tot} is close to 1, the bias is significant when N is only slightly larger than k. The closer the sample size is to k, the larger the overestimation of R^2, or the closer R^2 is to its upper limit of 1. Note that the sample size N still needs to be larger than k to allow the calculation of the unadjusted R^2. Since all curves decrease with increasing R^2 and end at a zero bias for R^2 = 1, a slight increase of the sample size to $1.5k$ or $2k$, for example, leads to a much smaller bias. Furthermore, it can be observed that the bias is close to negligible if the sample size is larger than k by a factor of 10 or more. When applying the adjustment to the group-wise R^2 of Section 2.2.1 in a calculation based on the 56-group covariance with a sample size of 1,000, N is almost 18 times larger than k, so the largest bias is small at less than 0.06.

Confidence interval. To express uncertainty due to sampling with a limited sample size, a confidence interval $\left[R^2 - q_{\alpha/2} \cdot \sigma, R^2 + q_{\alpha/2} \cdot \sigma\right]$ for R^2 (Olkin and Finn, 1995; Cohen, 2003) can be determined using the standard deviation:

$$\sigma = \sqrt{\frac{4R^2\left(1-R^2\right)^2(N-k-1)^2}{\left(N^2-1\right)(N+3)}}. \tag{11}$$

For 95% confidence, $q_{\alpha/2} = 1.96$ is the corresponding quantile of the normal distribution. The development of the 95% confidence interval as a function of R^2 is presented in Fig. 2. Due to the symmetry of the confidence interval, only the upper confidence level is presented. The figure shows a rapid increase in the relative confidence interval for R^2 for correlation coefficients below about 0.3. It is interesting to note that the R^2 confidence interval for k = 56 is larger than the corresponding interval for k = 252. This is counterintuitive since the degrees of freedom are reduced for larger k. This is the result of the term $(N-k-1)^2$ in Eq. (11): If k is decreasing for a constant N, then this term becomes larger, resulting in a larger σ. Another counterintuitive result of this term is that for $k > 225$, the confidence interval is smaller for $N = 500$ than for $N = 1000$.

Significance level. The significance level of R^2 is determined using the assumption that the multiple correlation is zero if the parameter group of interest is insignificant for the system under consideration or if the output is independent of the sampled input parameters. In this case, R^2 follows the beta distribution with $p = k$ and $q = N - k - 1$ (Müller, 1980). The 95% significance level (α = 0.95), which is the level at which the hypothesis that R^2 is independent of the perturbed input parameters is rejected, is therefore calculated using the inverse cumulative beta distribution function:

$$R^2_{sign} = BetaCDF^{-1}(\alpha; p, q) = BetaCDF^{-1}\left(0.95; \frac{k}{2}, \frac{N-k-1}{2}\right). \tag{12}$$

This is valid if the input parameters are normally distributed. While the pure calculation of R^2 is possible if the sample size N is larger than k, it does not mean that the obtained R^2 value is statistically significant. Each calculated R^2 value should be tested for statistical significance by comparing its value with the determined statistical significance level.

The development of the 95% significance level as a function of the sample size is presented in Fig. 3. Given that R^2 values are often smaller than 0.5 (see Chapter 4), this figure suggests that a sample size larger than 200 is required for cases with $k = 56$ and a sample size larger than 600 is required for cases with $k = 252$ to obtain at least one statistically relevant R^2 value above the significance level. If smaller sample sizes are chosen, then it is possible that not a sin-

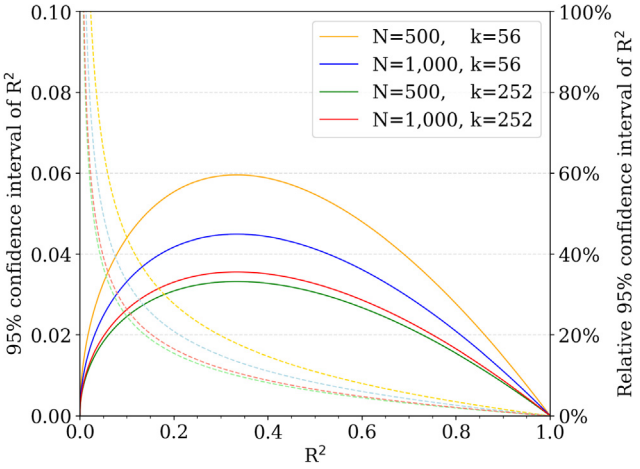

Fig. 2. 95% confidence interval of R^2 for two different samples sizes N and number of independent parameters k (solid lines indicate absolute confidence intervals; dashed lines indicate relative confidence intervals).

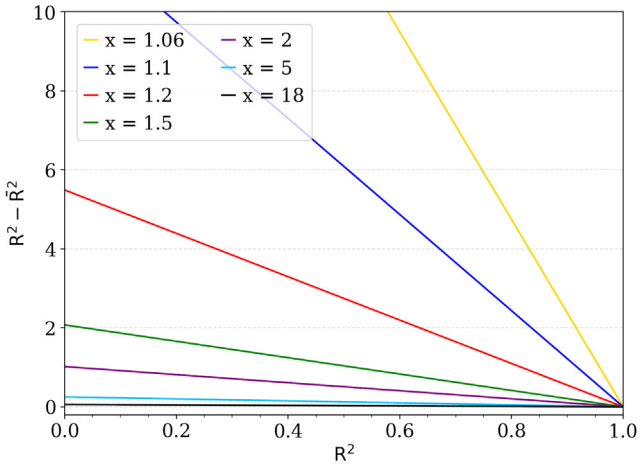

Fig. 1. Difference between R^2 and the corresponding adjusted value $\overline{R}^2$ as a function of R^2 for sample sizes $N = x \cdot k$, with k = 56.

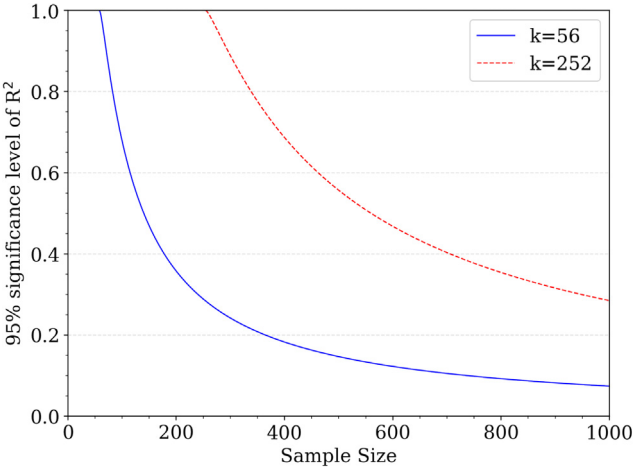

Fig. 3. 95% significance level of R^2 for two different numbers of independent parameters k.

gle calculated R^2 value is statistically relevant (that is, above the significance level and therefore clearly outside of statistical noise).

With a sample size of 1,000 and $k = 56$, usually 5–10 statistically significant R^2 values are obtained. If more statistically significant R^2 values are desired, then the significance level needs to be reduced by increasing the sample size. Sample sizes larger than 1,000 are also needed to obtain statistically relevant R^2 values for applications with covariance libraries with many energy groups (that is, with $k > 56$, as for example with $k = 252$).

2.2.2. SPC^2 – squared semi-partial multiple correlation coefficient

As in the incremental sensitivity index ST_A, an additional importance indicator with a different interpretation can be determined as a linearized version of ST_A. The so-called *squared semi-partial multiple correlation coefficient*, or SPC^2_A, for a parameter group A is defined as follows (Glaeser, 2008, 2012):

$$SPC^2_{Y,A} = R^2_{Y,A+B} - R^2_{Y,B}. \tag{13}$$

$R^2_{Y,A+B}$ is the total squared multiple correlation coefficient between the output Y and all parameters A and B, and $R^2_{Y,B}$ is the squared multiple correlation coefficient between the output Y and the complementary group B. Due to the subtraction of these two coefficients, $SPC^2_{Y,A}$ is sometimes also called *incremental* R^2. It is a measure of the linear dependency between the output Y and the input parameter group A after excluding linear influences of the complementary group B on group A. Influences of the complementary parameter group on the output still remain (Glaeser, 2012). Analogous to the interpretation of ST_A, $SPC^2_{Y,A}$ describes the variance of the output quantity which is expected to remain when the true values of the complementary parameter group B become known (Glaeser, 2008). In other words, $SPC^2_{Y,A}$ is the fraction of the variance that group A adds to the variance caused by group B (Glaeser, 2012).

As with R^2, SPC^2 can also be determined from the results of a single set of calculations for any group of parameters. However, the sample size must be larger than the number of parameters considered for the determination of $R^2_{Y,A+B}$ and $R^2_{Y,B}$. Since $R^2_{Y,A+B}$ is the *total* multiple correlation coefficient, the sample size must be significantly larger than the *total* number of sampled parameters that are relevant for the system under consideration. For a simple problem with only a few nuclides, the required sample size can be in the range of a few thousands.

Confidence interval. With the sample size N and the quantile of the normal distribution $q_{\alpha/2}$, the confidence interval of SPC^2 is as follows (Algina, 2008):

$$\left[SPC^2_{Y,A} - q_{\alpha/2}\cdot\sigma, SPC^2_{Y,A} + q_{\alpha/2}\cdot\sigma\right], \tag{14}$$

where

$$\sigma = \sqrt{\phi_f + \phi_r - 2 * \phi_{fr}}, r_{ab} = \sqrt{\frac{R^2_{Y,B}}{R^2_{Y,A+B}}},$$
$$\phi_f = \frac{4}{N}R^2_{Y,A+B}\left(1 - R^2_{Y,A+B}\right)^2, \phi_r = \frac{4}{N}R^2_{Y,B}\left(1 - R^2_{Y,B}\right)^2,$$
$$\phi_{fr} = \frac{4}{N^2}\sqrt{R^2_{Y,A+B}R^2_{Y,B}}\left[\frac{1}{2}\left(2r_{ab} - \sqrt{R^2_{Y,A+B}R^2_{Y,B}}\right)\left(1 - R^2_{Y,A+B} - R^2_{Y,B} - r^2_{ab}\right) + r^3_{ab}\right].$$

Note that the calculation of the confidence interval is performed without consideration of the number of independent parameters k. Fig. 4 shows that the confidence interval for SPC^2 is much larger than for R^2; a large sample size is needed to obtain statistically relevant values for SPC^2.

Adjusted SPC^2. When considering the adjustment of R^2 using Eq. (10), it is possible to derive an adjusted SPC^2 based on Eq. (13) to consider the limited degrees of freedom:

$$\overline{SPC}^2_{Y,A} = \overline{R}^2_{Y,A+B} - \overline{R}^2_{Y,B}. \tag{15}$$

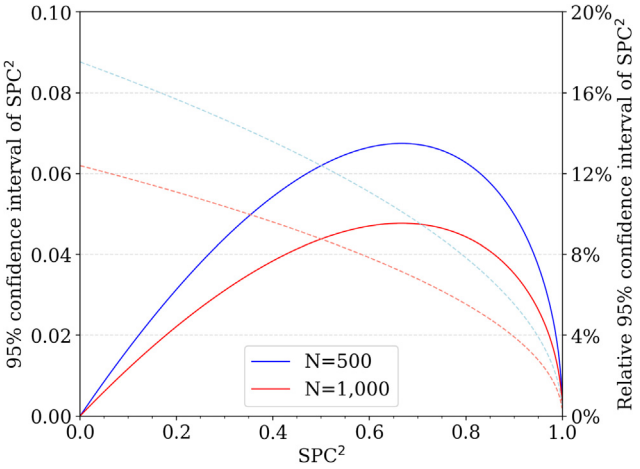

Fig. 4. 95% confidence interval of SPC^2 for two different samples sizes N, assuming $R^2_{Y,A+B} = 1$ (solid: absolute confidence intervals; dashed: relative confidence intervals).

For a large total number of independent parameters k in the calculation, it is reasonable to assume that the number of independent parameters considered in the calculations of $\overline{R}^2_{Y,A+B}$ and $\overline{R}^2_{Y,B}$ is approximately identical because the maximum difference is the number of energy groups in the covariance library. With this assumption, it is possible to estimate the adjustment as follows:

$$\overline{SPC}^2_{Y,A} \approx \left(R^2_{Y,A+B} - R^2_{Y,B}\right)\left(\frac{N-1}{N-k-1}\right). \tag{16}$$

2.3. Differentiation from top contributors in perturbation theory

In first-order perturbation theory, the derivatives of the output quantity Y with respect to the input parameters—in this case, cross sections Σ—are obtained for all nuclides i of the model of interest with all reactions x in all energy groups g:

$$S_{Y,\Sigma^i_{x,g}} = \left(\frac{\Sigma_i}{Y}\frac{\mathrm{d}Y}{\mathrm{d}\Sigma^i_{x,g}}\right). \tag{17}$$

$S_{Y,\Sigma^i_{x,g}}$ are often called *sensitivity coefficients*. (Note: It is important not to confuse these sensitivity coefficients with the *sensitivity indices* R^2 and SPC^2.) The sensitivity coefficients are obtained using first-order perturbation theory as described in detail by M. Williams (Williams, 1986; Williams et al., 2001). $S_{Y,\Sigma^i_{x,g}}$ describes the impact of a perturbation of cross section x of nuclide i in energy group g on the output quantity Y.

The nuclear data uncertainties are given in energy-dependent covariance matrices for each nuclide reaction and for correlations between different nuclide reactions. Using these covariance matrices and the sensitivity coefficients, the application of first-order uncertainty propagation (the so-called *sandwich formula*) leads to the total output variance:

$$\sigma^2_Y = \mathbf{S}^T_{Y,\Sigma}\,\mathbf{C}\,\mathbf{S}_{Y,\Sigma}. \tag{18}$$

Vector $\mathbf{S}_{Y,\Sigma}$ includes the sensitivities of all the input cross sections to the output quantity, and the covariance matrix $\mathbf{C}$ includes the covariance matrices of all the input cross sections.

If Eq. (18) is applied to only the covariance matrix of parameter group A, then the individual contribution of group A to the output uncertainty is obtained. However, the output of this expression only corresponds to the total contribution of parameter group A

to the output uncertainty if this parameter group is independent of all other parameter groups, or if there is no correlation of the investigated nuclide reaction to other nuclide reactions. As soon as there are correlations between parameter groups (i.e., between nuclide reactions), this expression is not suitable for describing the total contribution of a nuclide reaction to the output uncertainty.

Often a list of individual contributions of all relevant covariance matrices (i.e. the contribution of the uncertainties of one nuclide reaction through its corresponding covariance matrix) is provided to the user. The contribution of the correlation between two nuclide reactions is listed as a separate record in the list of contributions. Since the individual contributions cannot be combined to obtain total contributions of nuclide reactions in practice, it is not possible to assess the total contribution of a nuclide reaction with an appropriate consideration or interpretation of correlations to other nuclide reactions. This gap is closed by the determination of R^2 and SPC^2.

2.4. Consistency between approaches

This work focuses on the demonstration of R^2 and SPC^2 as implemented in the SCALE's Sampler sequence. The calculation of Sobol' main effect and total effect sensitivity indices was previously demonstrated and shown to provide almost consistent results with R^2 and SPC^2 (Bostelmann, 2020). The same study also developed and demonstrated corresponding indices that are calculated using sensitivity coefficients from perturbation theory. Also for these indices, consistent results with R^2 and SPC^2 were obtained.

3. Codes and models

Sampler's new sensitivity analysis is demonstrated by analyzing the development of the eigenvalue and the decay heat of a typical BWR fuel assembly. In the following, the BWR assembly model and the applied tools and nuclear data libraries are described.

3.1. Boiling water reactor fuel assembly

The BWR fuel assembly model used in this study is taken from a previous study by G. Ilas and H. Liljenfeldt in which Sampler was used to quantify the effect of uncertainties in nuclear data and selected manufacturing and operation parameters on calculated decay heat (Ilas and Liljenfeldt, 2017). The availability of high-quality decay heat measurements for the studied BWR assembly enabled an assessment of the significance of the results through comparison of calculated with measured decay heat data.

The 8 × 8 BWR assembly has an average discharge burnup of 36.9 GWd/MTIHM (MTIHM: metric ton initial heavy metal. The assembly includes 63 fuel rods—59 regular fuel (UO_2) rods, 4 gadolinia (UO_2-Gd_2O_3) rods, and one water rod (Fig. 5). The assembly has fuel rods with five enrichments: 1.38, 1.98, 2.49, 3.17, and 3.37 wt% ^{235}U. Unique colors in Fig. 5 indicate the rods' unique enrichment values, and the white rod represents the water rod. The rods shown with multiple rings are the gadolinia rods. Details for the measurements and the assembly, which is labeled as 6432R1, can be found in Sturek (Sturek et al., 2006).

The decay heat of the selected BWR assembly was measured at the Swedish Central Interim Storage Facility for Spent Nuclear Fuel (Clab) as part of a comprehensive experimental program initiated and managed by Svensk Kärnbränslehantering AB (SKB), the Swedish Nuclear Fuel and Waste Management Company. Sturek provides experimental decay heat data for this assembly from 10 measurements performed over a period of almost 6 years that correspond to cooling times between 14.8 and 20.6 years (Table 1)

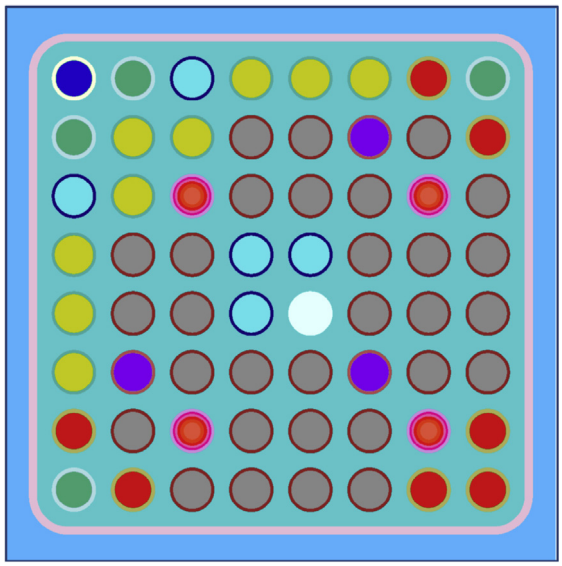

Fig. 5. SCALE model of the 6432R1 BWR assembly (Ilas and Liljenfeldt, 2017).

Table 1
Measured and calculated decay heat for assembly 6432R1. The measured data are provided along with the corresponding 1σ uncertainty (Sturek et al., 2006). The difference is provided in Watt and in multiples of the measured uncertainty σ.

Cooling time [days]	Measurement [Watt]	Calculation [Watt]	Difference [Watt]
5422	185.48 ± 2.55	186.04	0.56 (0.2 σ)
5424	189.55 ± 2.57	186.04	−3.51 (1.4 σ)
5670	184.44 ± 2.55	183.38	−1.06 (0.4 σ)
5680	182.79 ± 2.54	183.20	0.41 (0.2 σ)
5681	185.17 ± 2.55	183.20	−1.97 (0.8 σ)
5687	181.63 ± 2.54	183.20	1.57 (0.6 σ)
5688	181.99 ± 2.54	183.20	1.21 (0.5 σ)
6425	175.92 ± 2.52	175.64	−0.28 (0.1 σ)
7521	161.72 ± 2.47	165.66	3.94 (1.6 σ)
7526	161.72 ± 2.47	165.63	3.91 (1.6 σ)

(Sturek et al., 2006). The reported measurement uncertainty at a 95% confidence level (2σ) is 4.2 W at 50 W decay heat and 6.2 W at 350 W decay heat. Assuming that the uncertainty varies linearly with the decay heat, the relative uncertainties of the measured data are between 1.35 and 1.53%.

3.2. Computational tools and nuclear data libraries

The uncertainty and sensitivity analyses were performed with the Sampler sequence (Williams et al., 2013) of the SCALE code system (Wieselquist et al., 2020). Sampler employs the random sampling approach by applying perturbations to cross sections used by any other SCALE sequence. SCALE's data library resource includes perturbation factors that were generated via conditional sampling based on the nuclear covariance data, so they only need to be multiplied with the corresponding nominal cross sections to arrive at perturbed cross sections. Sampler automatically runs a specified number of realizations of this sequence with perturbed data and performs the statistical analysis of the results. The analysis of R^2 and SPC^2 was recently added to the statistical analysis. The user requests the calculation of either R^2 or SPC^2, provides the output quantities of interest, and lists the nuclides for which a sensitivity analysis is desired. The requested sensitivity index is then calculated for all reactions of the specified nuclides. The results are pro-

vided with their corresponding statistical confidence intervals and ranked according to size to allow for clear identification of relevant nuclide reactions.

The individual BWR fuel assembly depletion calculations were performed with SCALE's reactor physics sequence TRITON. By calling various modules in SCALE, TRITON controls the following steps: (1) generation of problem-dependent cross sections through XSProc, (2) neutron transport calculation with one of SCALE's neutron transport kernels, and (3) depletion/decay calculations through the depletion/irradiation/decay solver ORIGEN. The neutron transport kernel used in this study is the two-dimensional deterministic code NEWT.

The TRITON-NEWT calculations were performed with the 252-group ENDF/B-VII.1 cross section library (Chadwick et al., 2011). Sampler applied perturbations to these cross sections that were generated using SCALE's 56-group ENDF/B-VII.1-based covariance library. This covariance library mainly contains data from the ENDF/B-VII.1 release, but it also contains (1) additional fission spectrum uncertainties from the JENDL 4.0 library (Shibata et al., 2012), (2) approximate uncertainties from the Low-fidelity Covariance Project,a collaboration of Brookhaven National Laboratory, Los Alamos National Laboratory, and Oak Ridge National Laboratory (Little et al., 2008), and (3) approximate covariance data from the Working Party on International Nuclear Data Evaluation Cooperation Subgroup-26 (Salvatores and Jacqmin, 2008). More details on these libraries can be found in the SCALE manual (Wieselquist et al., 2020).

The BWR fuel assembly was depleted up to the discharge burnup of 36.9 GWd/MTIHM, followed by calculation of the decay heat up to 10,000 years after discharge. Sampler was applied with a sample size of 1,000. An uncertainty and sensitivity analysis was performed for the eigenvalue k_{eff} during depletion, and it was also performed for the decay heat during cooling. The new sensitivity analysis is currently limited to the analysis of cross section uncertainties, so fission yield and decay data uncertainties were not taken into account.

To stress the difference of the Sampler's new sensitivity indices R^2 and SPC^2 to the commonly studied top contributing nuclide reactions from perturbation theory, TSUNAMI (Broadhead et al., 2004; Rearden et al., 2011) calculations were additionally performed for the initial criticality of the BWR assembly. Just as for the Sampler calculation, TSUNAMI was used in combination with the NEWT neutron transport code. TSUNAMI provides the total eigenvalue uncertainty as well as the individual contributions to the uncertainty by multiplying the sensitivities of the individual nuclide reactions with their corresponding covariance matrix. The same nuclear data libraries as for the Sampler calculations were applied.

All analyses were performed with codes and nuclear data libraries from a pre-release version of SCALE 6.3.

4. Application

Sampler's sensitivity analysis is first demonstrated for the BWR fuel assembly eigenvalue k_{eff} during depletion, followed by the analysis of the decay heat during cooling.

4.1. Eigenvalue analysis

4.1.1. Uncertainty analysis

Fig. 6 presents the eigenvalue k_{eff} of the BWR fuel assembly and the corresponding uncertainty during depletion. The first dip in the k_{eff} after a few days is the result of the buildup of the neutron poison xenon, and the subsequent increase of k_{eff} up to ~300 days is the result of the depletion of the neutron poison gadolinium in the UO_2-Gd_2O_3 fuel pins.

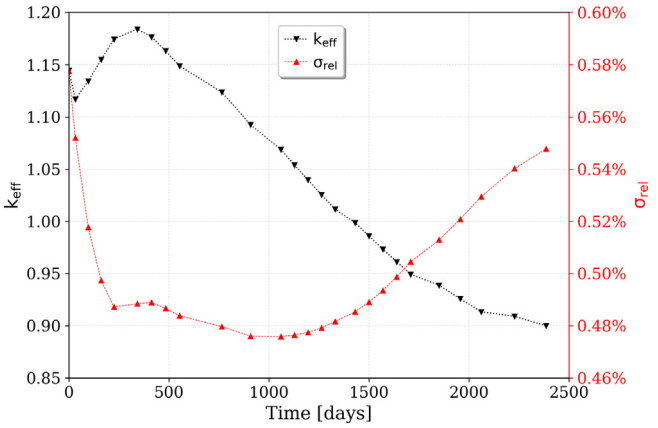

Fig. 6. Development of eigenvalue and corresponding relative uncertainty over the course of depletion.

The k_{eff} uncertainty is about 0.5% throughout depletion, as shown in many previous studies (Aures et al., 2017; Rochman et al., 2017). The decrease of uncertainty during the first 200 days is the result of decreasing influences of ^{235}U cross sections due to the depletion of ^{235}U. The increase of uncertainty over the second half of the depletion can be explained by the increasing relevance of plutonium cross sections due to plutonium buildup. The sensitivity analysis in terms of R^2 and SPC^2 can be used to confirm this explanation and to identify the relevant uranium and plutonium reactions.

The k_{eff} uncertainty obtained with TSUNAMI at beginning of life is 0.600% as compared to the uncertainty of 0.578% obtained with Sampler. Considering the statistical uncertainty of the Sampler's uncertainty, this is good agreement.

4.1.2. Sensitivity analysis $\Delta k/k$

Fig. 7 presents the top contributors to the eigenvalue uncertainty at beginning of depletion as obtained with TSUNAMI. The individual contributions are the results of the multiplication of the sensitivity coefficients with the reaction and the corresponding covariance matrix. The contribution "U-235 fis/n,γ" indicates the

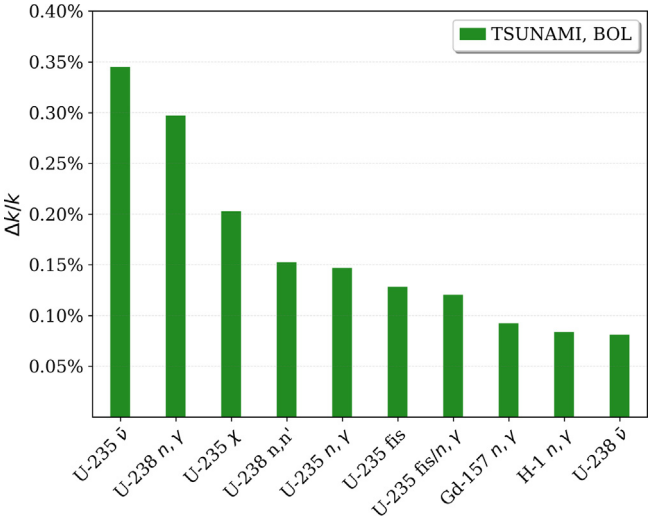

Fig. 7. Contributors to eigenvalue in terms of $\Delta k/k$ at the beginning of depletion obtained with TSUNAMI.

contribution of the correlation between fission and radiative neutron capture (n,γ) of ^{235}U. Since the model contains fresh fuel at beginning of depletion, the major contributors are reactions of ^{235}U and ^{238}U.

4.1.3. Sensitivity analysis R^2

As stated in Section 2.2, the calculation of R^2 mathematically requires a sample size larger than the number of independently sampled parameters k in the reaction of interest (parameter group). If this requirement is not met, SCALE stops with a corresponding error message. Furthermore, a small significance level is desired to allow the identification of at least a few statistically significant R^2 values. SCALE provides a list of R^2 values along with the corresponding confidence intervals and significance levels. The user can analyze these results to identify statistically relevant R^2 values (for example, by comparing the value with the significance level) or to estimate a required larger sample size that would lead to additional statistically relevant R^2 values.

Since the Sampler calculation was performed with perturbations based on a covariance library with 56 energy groups, k is equal to or less than 56. k is less than 56 if only a subset of the cross sections of a reaction is sampled independently. This is the case either if strong positive or negative correlations between the cross sections exist such that only one of the correlated cross sections is sampled, or if the variance of a cross section in an energy group is zero. The sample size chosen for this calculation was 1,000 and therefore meets the requirement for the calculation of R^2. Given the development of the significance level in Fig. 3, this sample size should also be sufficient to identify at least a few statistically significant R^2 values.

Figs. 8 and 9 present the sensitivity index R^2 for the reactions with the largest obtained R^2 values at the depletion's beginning of life (BOL) and end of life (EOL). The error bars indicate a 95% confidence interval of R^2. The light columns on top of the dark columns indicate the 95% significance bounds of R^2. If the obtained value for R^2 is below this level, then it might be the result of statistical noise and cannot be considered statistically relevant. For example, R^2 for ^{239}Pu (n,γ) is below the significance bound at BOL, but it shows a clearly significant value at EOL. This makes sense because plutonium is only building up over the course of depletion. The applied sample size of 1,000 in the present example results in 5–10 statistically significant R^2 values throughout depletion. If it was desired to study reactions with smaller relevance for the analyzed output quantity, then the sample size would need to be increased to reduce the significance level and thereby to allow smaller statistically relevant R^2 values.

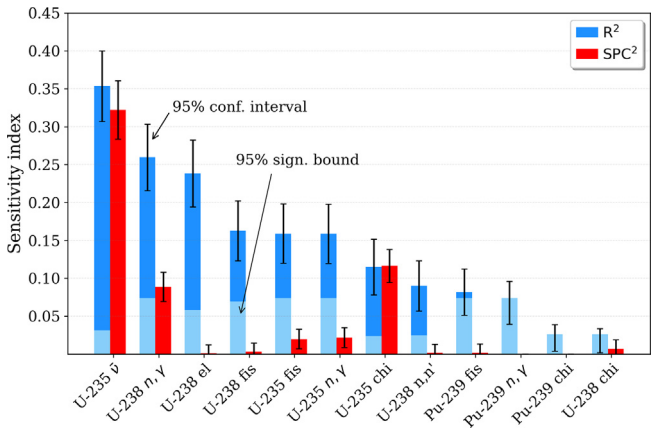

Fig. 8. Eigenvalue R^2 and SPC^2 at the beginning of depletion.

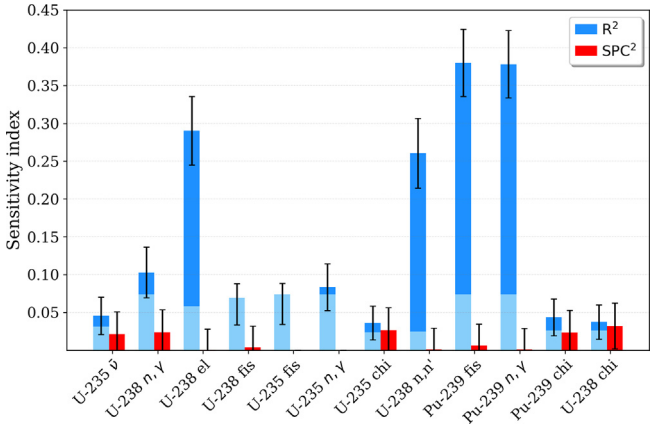

Fig. 9. Eigenvalue R^2 and SPC^2 at the end of depletion.

The occurrence of an R^2 for ^{239}Pu for fresh uranium fuel at BOL—even though statistically insignificant—stresses an interesting fact about R^2: R^2 can be calculated for any reaction of any nuclide; it is not relevant whether the nuclide is included in the input model (i.e., included in the composition of any mixture). Although it is unlikely that nuclides excluded from the model would result in statistically significant indices, in theory, this could occur in the case of correlations to an important reaction of a nuclide that is included in the model. In ENDF/B-VII.1, correlations between reactions of different nuclides exist, for example, for ^{197}Au and ^{235}U, and also between ^{238}U and ^{239}Pu. Is it worth pointing out that correlations between reactions cannot be excluded during the calculation of R^2 since the calculation of R^2 does not explicitly consider those correlations (see Section 2.2). Correlations are indirectly considered through the generation of the perturbed cross sections during the conditional sampling which considered all correlations available in the covariance library. If certain correlations are desired to be excluded, then the cross section sampling would need to be modified.

The most important contributor to the k_{eff} uncertainty at BOL as identified using R^2 is the neutron multiplicity $\bar{\nu}$ of ^{235}U. This is reasonable because of the immediate influence of $\bar{\nu}$ on k_{eff} and it is also consistent with the results from the TSUNAMI calculation. In general, the identified top nuclear reactions are consistent between Sampler and TSUNAMI at BOL. At EOL, the buildup of plutonium isotopes during depletion causes a large contribution of the ^{239}Pu fission and (n,γ) reaction to the k_{eff} uncertainty. Fig. 10 shows the top contributors to the k_{eff} uncertainty during depletion, clearly indicating the decreasing influence of ^{235}U $\bar{\nu}$ while ^{235}U is depleting, as well as an increasing influence of ^{239}Pu reactions while plutonium is building up.

It must be stressed again that the top contributors result from (1) a significant sensitivity of k_{eff} to a reaction and (2) a simultaneous relevant uncertainty of this reaction. Unexpectedly large contributions are identified for ^{238}U elastic and inelastic scattering. One-at-a-time perturbations of the individual reactions have demonstrated that contributions in terms of R^2 can be overestimated because of correlations between reactions (Bostelmann, 2020): A reaction can show a large R^2 value only because of the relevance of a highly correlated reaction. It is consequently possible that the importance of ^{238}U elastic and inelastic scattering is increased due to their correlations with each other as well as correlations to the ^{238}U fission and (n,γ) reaction.

4.1.4. Sensitivity analysis SPC^2

The calculation of SPC^2 mathematically requires a sample size larger than the total number of independently sampled parameters

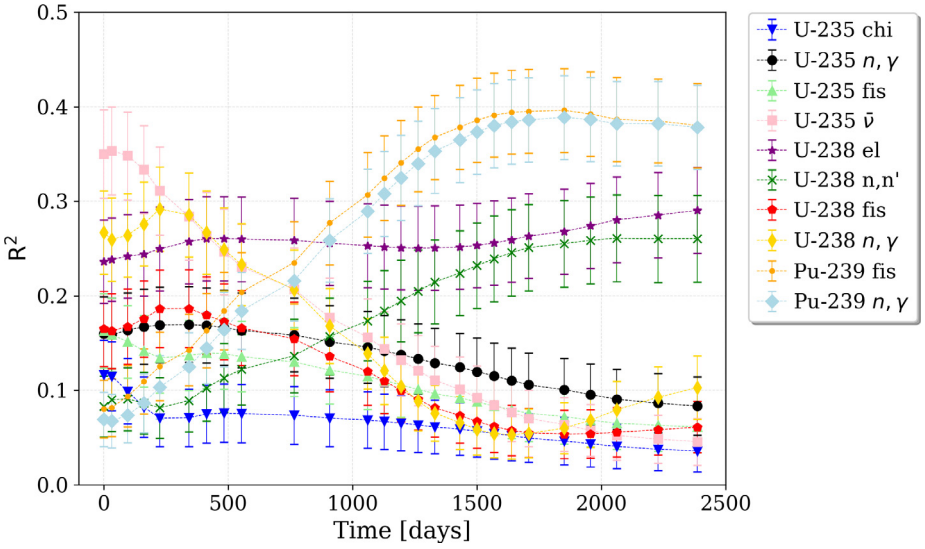

Fig. 10. Eigenvalue R^2 during depletion.

k in the problem. If this requirement is not met, SCALE stops with a corresponding error message. In this particular calculation, 220 nuclides were considered in the neutron transport calculations to determine k_{eff}. Consequently, 220 nuclides—for which all reactions are given in always 56 energy groups—must be considered. This requires a sample size of several thousand. Since the impact of most reactions on k_{eff} is insignificant, the group of considered nuclides can be reduced to allow a calculation of SPC^2 with a reduced sample size. It has been shown that an appropriate selection of the considered nuclides leads to good agreement with results obtained with the full set of nuclides (Bostelmann et al., 2018). Based on the results for R^2 above, only ^{235}U, ^{238}U, and ^{239}Pu were considered in this SPC^2 calculation. This resulted in the consideration of in total 25 reactions, or 667 independent parameters, which is below the chosen sample size of 1,000. SCALE provides a list of unadjusted and adjusted SPC^2 values along with the corresponding confidence intervals. The user can analyze these results to identify statistically relevant SPC^2 values (for example, values for which the value is larger than the confidence interval) or to estimate a required larger sample size that would lead to additional statistically relevant SPC^2 values. Only adjusted SPC^2 results are presented here: that is, results considering the limited sample size and the number of sampled parameters.

Since the calculation of the total sensitivity index R^2_{tot} is required for the calculation of SPC^2, Sampler provides this index along with each SPC^2 calculation. R^2_{tot} is considered here as an indicator to assess whether the most important contributors were considered in the analysis. At BOL, R^2_{tot} was found to be $\sim 0.977 \pm 0.001$. This decreased slightly to $\sim 0.942 \pm 0.003$ at EOL, indicating that this choice of nuclides accounts for 98% of variance at BOL and 94% at EOL; therefore, it is concluded that the selection of nuclides captures the most relevant contributions to the k_{eff} uncertainty. If this calculation was repeated under consideration of all nuclides based on a calculation with a larger sample size, an assessment of the impact of nonlinear effects on the output uncertainty as described in Section 2.2 and shown by (Bostelmann, 2020) could be performed.

Figs. 8 and 9 include the sensitivity index SPC^2 for the reactions with the largest obtained SPC^2 values at the depletion's BOL and EOL, comparing them to the corresponding R^2 values. Fig. 11 shows the development of SPC^2 for these reactions during depletion. The error bars indicate the 95% confidence interval of SPC^2. A general observation is the absence of elastic and inelastic scattering of ^{238}U can be seen among the contributors. This result can be

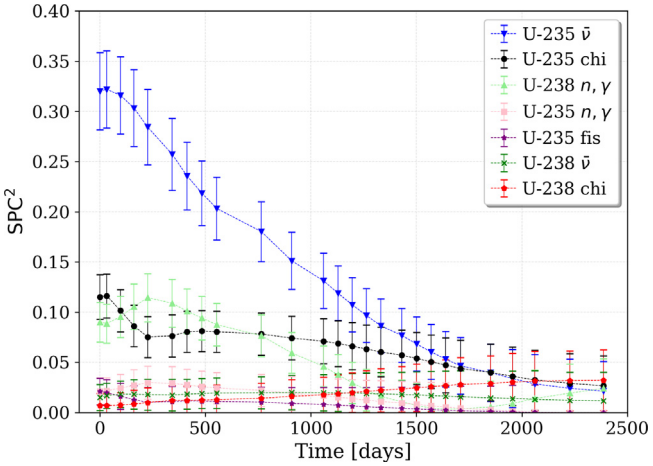

Fig. 11. Eigenvalue SPC^2 during depletion.

explained using the interpretation of SPC^2: SPC^2 indicates the contribution to the output variance by an individual nuclide reaction that is added when contributions of all other nuclide reactions (the complementary group) are already considered. Due to strong correlations between elastic and inelastic scattering of ^{238}U, the additional contribution of one of these reactions is negligible. For example, when investigating the additional contribution of ^{238}U inelastic scattering to the output variance, the contribution of this reaction is already considered by ^{238}U elastic scattering in the complementary group due to correlations. Consequently, the additional effect is small.

The second general observation is the clear identification of five top contributors at BOL, while no statistically relevant SPC^2 indices were obtained at EOL. This result can be explained by the large number of reactions that influence the k_{eff} uncertainty at EOL due to the buildup of fission products and actinides during depletion. It is challenging to identify an individual influence among all small contributions; this can only be simplified by a dramatic increase of the sample size.

The absence of the main contributor to the uncertainty in the ranking of SPC^2 stresses that SPC^2 cannot clearly reveal the top contributors to the output uncertainty. It can only be used in addi-

tion to the analysis with R^2. For example, relevant correlations between reactions can be identified by their absence in the SPC^2 ranking (see ^{238}U inelastic and elastic scattering contributions in terms of R^2, but missing contributions in terms of SPC^2 in Fig. 8). Correlations often exist between reactions of a nuclide or between reactions of different nuclides. Without the additional SPC^2 analysis, it is not necessarily clear which correlation between reactions is significant for the observed output uncertainties. However, such an analysis is to cases in which multiple statistically relevant SPC^2 are obtained. In the provided example, this analysis is possible at BOL, but not at EOL.

4.2. Decay heat analysis

4.2.1. Uncertainty analysis

Fig. 14 presents the calculated decay heat of the BWR fuel assembly and the corresponding uncertainty during decay after discharge from the reactor. As expected, the decay heat is rapidly decreasing over the first few years, mainly due to the decay of short-lived fission products and their daughters. Up to a cooling time of ~10 years, fission products are responsible for 75–90% of the decay heat (Fig. 12). Afterwards, the contribution of actinides is increasing. From ~300 years on, actinides—mainly plutonium and americium isotopes—are responsible for almost 100% of the decay heat (Fig. 13). As already shown by Ilas and Liljenfeldt (Ilas and Liljenfeldt, 2017), the calculated decay heat is in excellent agreement with the measured values (Table 1). All calculated values agree within 2σ measurement uncertainties.

Fig. 14 also shows the calculated relative uncertainty of the decay heat due to uncertainties in nuclear data. However, the small uncertainty of less than 0.2% during the first day of decay and the increasing uncertainty up to ~1.7% at ~300 years can be misleading. Due to the rapid decrease in decay heat during cooling, the absolute uncertainty should be considered rather than the relative uncertainty. Fig. 15 shows that the absolute uncertainty is smaller than 10 W and therefore is already negligible after ~100 days. Even 1 s after discharge, when the decay heat is ~72.5 kW, the uncertainty of the decay heat is only 75 W. At the time of the measurement, the calculated uncertainty is approximately 1.5 W which might explain a part of the small discrepancy between the measurement and the calculation.

4.2.2. Sensitivity analysis R^2

The calculation of R^2 is performed to identify the top contributing reactions to the decay uncertainty. This analysis is independent of the output quantity and must only meet requirements with respect to the number of considered nuclides and the sample size. Therefore, with the same explanation as for k_{eff} above, the sample size is sufficient to obtain a small number of statistically relevant R^2 values. It shall be stressed here that the decay heat uncertainty

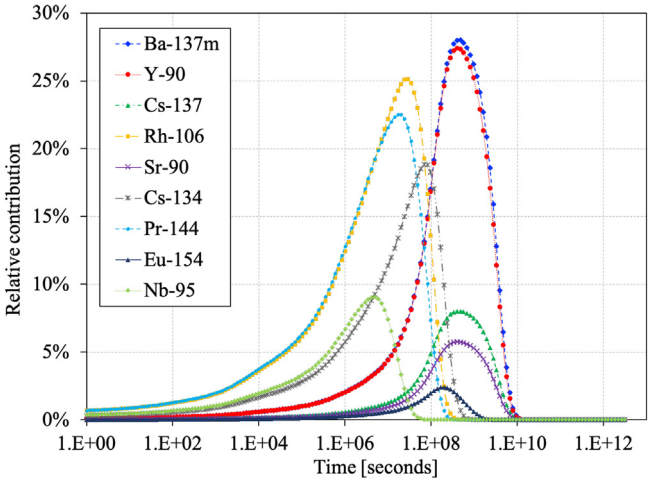

Fig. 12. Relative contribution of fission products to decay heat.

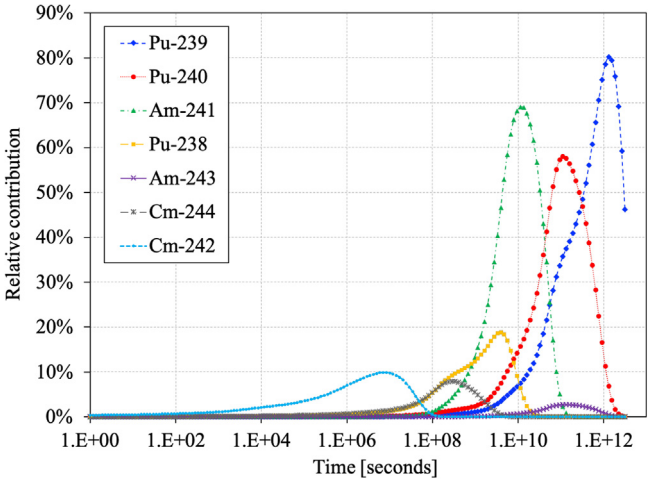

Fig. 13. Relative contribution of actinides to decay heat.

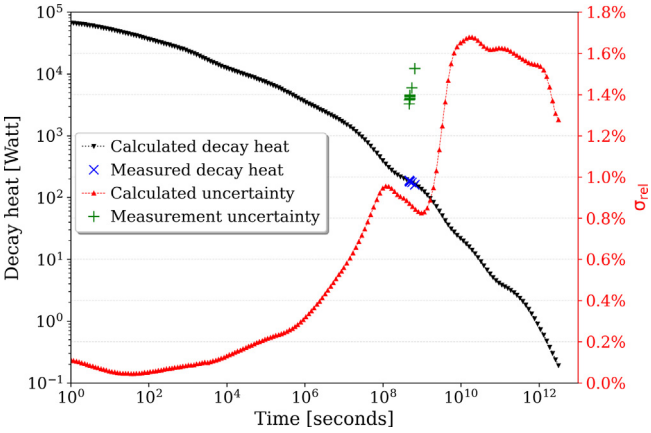

Fig. 14. Measured and calculated decay heat up to 10,000 years after discharge along with the measurement uncertainty and the calculated uncertainty resulting from uncertainties in nuclear data.

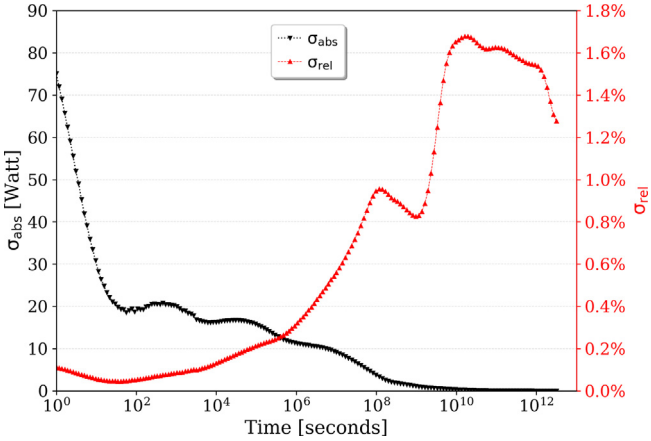

Fig. 15. Absolute and relative decay heat uncertainty as a function of cooling time.

is a quantity that cannot be easily investigated using perturbation theory–based approaches. Only the random sampling approach with a corresponding sensitivity analysis can be used to efficiently calculate quantities like the decay heat uncertainty and to analyze the contributors to the observed uncertainty.

Figs. 16 and 17 present the development of the top contributing reactions over the cooling time. Due to the varying contributions to the decay heat during decay, the contributors to the observed decay heat uncertainties also differ. Almost identical contributions of elastic and inelastic scattering of ^{238}U are observed immediately after discharge. It is assumed that the R^2 index for elastic scattering is only large because of a significant contribution of inelastic scattering. The decay heat immediately after discharge is dominated by fission products with very short half lives; their abundance is influenced by fission yields, decay constants, and the energy released per fission through the applied power. Because these data were not perturbed for the current calculation, these effects are not considered here. The occurrence of ^{238}U scattering reactions as relevant immediately after discharge is therefore assumed to be a second-order effect that is highlighted due to negligence of the most relevant effects at this point in time (see also Chapter 6). Furthermore, the number of short-lived fission products is very large, so the contribution of their uncertainties to the total decay heat uncertainty is spread over a large number of nuclides, resulting in small individual values for R^2.

Of the fission products, only the contribution of ^{133}Cs (n,γ) is notable. The uncertainty of this reaction directly influences the production of ^{134}Cs, a relevant contributor to the overall decay heat. The magnitude of R^2 for ^{133}Cs (n,γ) is consequently following the relative contribution of ^{134}Cs to decay heat in Fig. 12.

Of the actinides, ^{238}U, ^{239}Pu, ^{242}Pu, and ^{241}Am show large R^2 indices for some periods of time. The ^{241}Am (n,γ) reaction influences the production of ^{242}Am, which decays to ^{242}Cm—another important decay heat contributor—with a half life of ~16 h. The ^{242}Pu (n,γ) reaction influences the production of ^{243}Pu which decays to ^{243}Am—a contributor to the decay heat with constant absolute contribution and therefore increased relevance over time—with a half life of ~5 h. Similarly, the increase of R^2 of the correlated fission and (n,γ) reactions of ^{239}Pu starting 3 years after discharge goes along with the increasing contribution of ^{241}Am to decay heat, and the increase of R^2 of ^{238}U (n,γ) and the correlated ^{238}U fission reaction starting ~30 years after discharge coincides with the increasing contribution of ^{239}Pu and ^{240}Pu to decay heat.

When considering the major contributors to the decay heat as shown in Fig. 12, it is notable that the reactions of the following relevant nuclides do not show any significant contribution to the

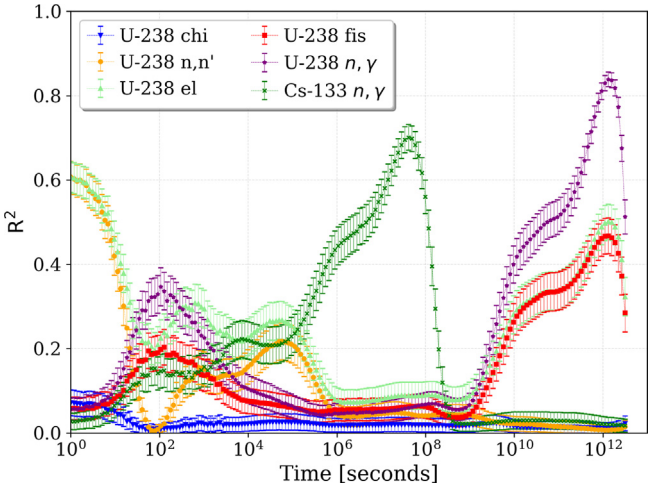

Fig. 16. Decay heat R^2 as a function of cooling time (set 1).

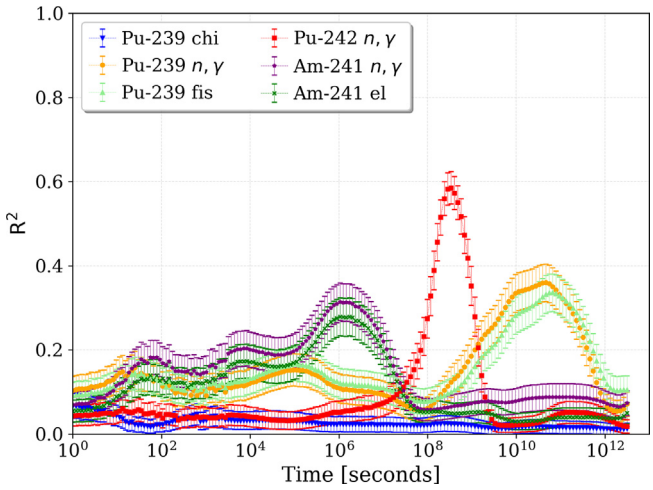

Fig. 17. Decay heat R^2 as a function of cooling time (set 2).

decay heat uncertainty through R^2: ^{90}Sr, ^{90}Y, ^{95}Nb, ^{106}Rh, ^{144}Pr, ^{137}Cs, and ^{137}mBa. ^{137}Cs is a direct fission product that β-decays into $^{137\ m}$Ba with a half life of ~30 years; ^{90}Sr is also a direct fission product that β-decays into ^{90}Y with a half life of ~28.9 years. ^{95}Nb and ^{106}Rh β-decay into stable nuclides with half lives of 35 days and 30 s, respectively. Since neither fission yield nor decay data uncertainties were considered in the analysis, but only cross section uncertainties, no significant R^2 values related to these isotopes were determined. ^{144}Pr is mainly the results of $^{144\ m}$Pr; since no covariance data are available in ENDF/B for either state of this nuclide, no corresponding R^2 values were calculated.

4.2.3. Sensitivity analysis SPC^2

As described above regarding k_{eff} and based on the R^2 decay heat results, the calculation of SPC^2 for the decay heat was performed under consideration of ^{133}Cs, ^{238}U, ^{239}Pu, ^{242}Pu, and ^{241}Am. This group of nuclides includes a total of 37 reactions with 853 independent parameters, which is below the sample size. The total correlation index R^2_{tot} during the SPC^2 calculation was found to be between 0.92 and 1.00 during decay. Since R^2_{tot} did not vary significantly from 1.0, it is concluded that the selection of nuclides captures the most relevant contributions to the decay heat uncertainty.

Fig. 18 shows the development of SPC^2 for these most important reactions during depletion. Just as for the SPC^2 of k_{eff}, some highly correlated reactions are missing among the contributors because the additional contribution to the output variance by some individual nuclide reactions is already considered by the corresponding complementary group of reactions. Reactions that are not (highly) correlated to any other reaction are still clearly showing up: for example, ^{133}Cs (n,γ).

Whereas 21 reactions were identified relevant at some point over the course of decay in terms of R^2, only 7 reactions were identified as statistically relevant in terms of SPC^2. This stresses again that SPC^2 is not to be used standalone, but it is useful to determine which of the results obtained for R^2 are most likely influenced by correlations between reactions.

5. Conclusions

SCALE's sequence for random sampling–based uncertainty analysis was extended by a sensitivity analysis in the form of two correlation-based sensitivity indices, the squared multiple correlation coefficient R^2, and the semi-partial squared multiple correlation coefficient SPC^2. In case of nuclear data uncertainty analysis, this sensitivity analysis allows for identification of the top contributing nuclear reactions to an observed output uncertainty.

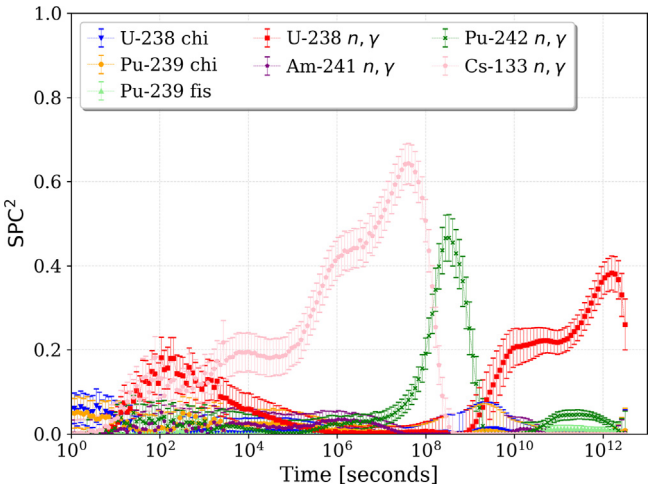

Fig. 18. Decay heat SPC^2 as a function of cooling time.

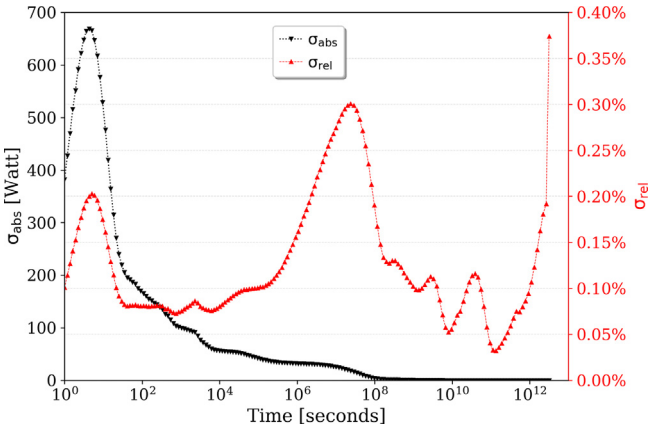

Fig. 19. Decay heat uncertainty due to decay data uncertainties during decay.

Therefore, it can be used to identify reactions for which a reduction of uncertainty through additional measurements or evaluations can significantly contribute to the reduction of the overall output uncertainties of interest. Since the random sampling approach allows the analysis of any output quantity of interest and is not limited to reaction rates and reactivities such as perturbation theory–based approaches, this analysis allows a sensitivity analysis of quantities like decay heat, as demonstrated in this work.

It was found that R^2 is the most practical and reliable sensitivity index that allows for identification of the major contributors to the output uncertainty. Due to consideration of the influence of correlated nuclide reactions, R^2 sometimes shows unexpected contributors. A common example is a large R^2 value for a scattering reaction due to the importance of correlated scattering or capture reactions. The analysis of SPC^2 can be used in some cases as a complementary analysis to identify important correlations since highly correlated nuclide reactions do not appear in the SPC^2 ranking. However, the calculation of SPC^2 with the random sampling approach requires either a very large sample size or the selection of a subgroup of nuclides to be considered in the analysis.

In the presented analysis of the fuel assembly eigenvalue during depletion and decay heat during cooling, the top contributing reactions to the observed output uncertainties could be clearly identified through R^2. In the case of the eigenvalue, the contributions of several ^{235}U reactions decreased over the course of depletion in favor of increasing contributions of ^{239}Pu reactions; this was as expected due to the depletion of ^{235}U and the buildup of plutonium isotopes. In the case of the decay heat, the top contributors that significantly vary over the cooling time could be attributed to the different nuclides' relative contribution to the decay heat. Many radiative capture reactions (n,γ) were found to be relevant because many relevant decay heat contributors are a result of this reaction—potentially with subsequent decay.

In conclusion, the analysis of R^2 provides a convenient means for identifying important nuclear reactions for an output uncertainty. Instead of performing computationally expensive one-at-a-time perturbations, this sensitivity analysis provides a time-efficient analysis as part of the post-processing—the statistical analysis of results. A certain expertise is needed to correctly interpret the results.

6. Outlook

The current implementation in Sampler is limited to the analysis of nuclear cross sections. However, there is also an impact of fission yield and decay data uncertainties in depletion calculations. The impact of fission yield uncertainties on the eigenvalue has been shown to be smaller than the impact of cross section uncertainties, and decay data uncertainties were found to be insignificant (Martinez et al., 2014). However, this is not necessarily true for other quantities.

In the fuel assembly study presented in this work, some relevant decay heat contributors did not show up in the R^2 ranking because these nuclides are direct fission products. If fission yield uncertainties were considered and the corresponding sensitivities could be determined, then significant contributions of the fission yields related to these nuclides are expected. With respect to the relevance of decay data, Fig. 19 shows the impact of decay data uncertainties on the decay heat of the fuel assembly. The initial peak a few seconds after discharge is caused by short-lived fission products; this peak of almost 700 W is significantly larger than the decay heat uncertainty due to nuclear cross sections at this time (less than 100 W).

These observations stress the need to consider all sources of uncertainties in decay heat analyses, including all sources of uncertainties in nuclear data. Other sources of uncertainties are parameters such as the geometry and material composition of a model which can be perturbed with Sampler. However, for such analyses, a sensitivity analysis has not yet been implemented. An exhaustive sensitivity analysis considering all of these sources of uncertainty can then help to clearly identify significant contributors to the uncertainty. Only then can this analysis be used to its full potential: to make the meaningful recommendations for further measurements and evaluations by correctly estimating the potential of an uncertainty reduction through the reduction in uncertainty of a limited number of input parameters. The extension of Sampler's current implementation of R^2 and SPC^2 to additional nuclear data and input parameters other than nuclear data is planned for a future release of SCALE.

CRediT authorship contribution statement

Friederike Bostelmann: Conceptualization, Methodology, Software, Validation, Formal analysis, Investigation, Resources, Data curation, Writing - original draft, Writing - review & editing, Visualization. **Dorothea Wiarda:** Software, Writing - review & editing, Supervision. **Goran Arbanas:** Methodology, Writing - original draft, Writing - review & editing. **William A. Wieselquist:** Conceptualization, Methodology, Software, Writing - review & editing, Supervision, Project administration, Funding acquisition, Resources.

Declaration of Competing Interest

The authors declare that they have no known competing financial interests or personal relationships that could have appeared to influence the work reported in this paper.

Acknowledgements

This work was supported by the US Nuclear Regulatory Commission Office of Nuclear Regulatory Research and the US Department of Energy Nuclear Criticality Safety Program. Dr. Ugur Mertyurek's (ORNL) comments and review of the implementation are much appreciated. The authors would like to thank Dr. Germina Ilas (ORNL) for providing her BWR fuel assembly model for the analysis in this paper. The discussions about XSUSA's sensitivity analysis with Dr. Winfried Zwermann (GRS), Prof. Andreas Pautz (École polytechnique fèdèrale de Lausanne), and Dr. Bernard Krzykacz-Hausmann (GRS) are also much appreciated.

Appendix A. Sobol's Main effect sensitivity index of a linear model

An expression for Sobol's Main effect sensitivity index SM_A of a linear model

$$Y(\Sigma) = E[Y] + c \cdot (\Sigma - E[\Sigma])^t \tag{A.1}$$

$$= E[Y] + a \cdot (\Sigma_A - E[\Sigma_A])^t + b \cdot (\Sigma_B - E[\Sigma_B])^t, \tag{A.2}$$

where $\Sigma = (\Sigma_A, \Sigma_B)$, and $c = (a, b)$ is a (constant) model sensitivity vector

$$c = \nabla_\Sigma Y(\Sigma)|_{\Sigma=E[\Sigma]} = \left(\nabla_{\Sigma_A}, \nabla_{\Sigma_B}\right) Y(\Sigma))|_{\Sigma=E[\Sigma]} = (a, b), \tag{A.3}$$

is derived by observing that

$$E[Y|\Sigma_A] = E[Y] + a \cdot (\Sigma_A - E[\Sigma_A])^t, \tag{A.4}$$

and

$$Var(E[Y|\Sigma_A]) = E\left[(E[Y|\Sigma_A] - E[Y])(E[Y|\Sigma_A] - E[Y])^t\right] \tag{A.5}$$

$$= E\left[a \cdot (\Sigma_A - E[\Sigma_A])^t (\Sigma_A - E[Y]) \cdot a^t\right] \tag{A.6}$$

$$= a \cdot E\left[(\Sigma_A - E[\Sigma_A])^t (\Sigma_A - E[Y])\right] \cdot a^t \tag{A.7}$$

$$= a \cdot Cov(\Sigma_A, \Sigma_A) \cdot a^t. \tag{A.8}$$

Together with an analogous expression for $Var(Y)$

$$Var(Y) = c \cdot Cov(\Sigma, \Sigma) \cdot c^t, \tag{A.9}$$

Eq. (1) can be written as

$$SM_A = \frac{a \cdot Cov(\Sigma_A, \Sigma_A) \cdot a^t}{c \cdot Cov(\Sigma, \Sigma) \cdot c^t}. \tag{A.10}$$

The expression for the squared multiple correlation coefficient $R^2_{Y,A}$ of a linear model is derived by rewriting Eq. (6) in matrix index notation:

$$R^2_{Y,A} = \sum_{ij} \boldsymbol{r}_{Y,i} \left[\mathbf{C}^{-1}_{AA}\right]_{ij} \boldsymbol{r}^t_{Y,j}, \tag{A.11}$$

where the summation is over the indices corresponding components of Σ_A, followed by expressing $\mathbf{r}_{Y,i}$ as

$$\boldsymbol{r}_{Y,i} = \frac{1}{\sqrt{Var(Y)}} Cov(Y, \Sigma_i) \frac{1}{\sqrt{Var(\Sigma_i)}} \tag{A.12}$$

$$= \frac{1}{\sqrt{Var(Y)}} \sum_k a_k Cov(\Sigma_k, \Sigma_i) \frac{1}{\sqrt{Var(\Sigma_i)}} \tag{A.13}$$

$$= \frac{1}{\sqrt{Var(Y)}} \sum_k a_k \sqrt{Var(\Sigma_k)} [\mathbf{C}_{AA}]_{ki}, \tag{A.14}$$

and, finally, inserting the expression above into Eq. (A.11) and using the expression for $Var(Y)$ in Eq. (A.9) to get

$$R^2_{Y,A} = \frac{\sum_{ijkl} a_k \sqrt{Var(\Sigma_k)} [\mathbf{C}_{AA}]_{ki} \left[\mathbf{C}^{-1}_{AA}\right]_{ij} [\mathbf{C}_{AA}]_{jl} \sqrt{Var(\Sigma_l)} a_l}{Var(Y)} \tag{A.15}$$

$$= \frac{\sum_{kl} a_k \sqrt{Var(\Sigma_k)} [\mathbf{C}_{AA}]_{kl} \sqrt{Var(\Sigma_l)} a_l}{Var(Y)} \tag{A.16}$$

$$= \frac{\sum_{kl} a_k Cov(\Sigma_k, \Sigma_l) a_l}{Var(Y)} \tag{A.17}$$

$$= \frac{a \cdot Cov(\Sigma_A, \Sigma_A) \cdot a^t}{c \cdot Cov(\Sigma, \Sigma) \cdot c^t} \tag{A.18}$$

which is equivalent to the corresponding expression for SM_A in Eq. (A.10).

References

Adams, B.M., Bohnhoff, W.J., Dalbey, K.R., Ebeida, M.S., Eddy, J.P., Eldred, M.S., Hooper, R.W., Hough, P.D., Hu, K.T., Jakeman, J.D., Khalil, M., Maupin, K.A., Monschke, J.A., Ridgway, E.M., Rushdi, A.A., Seidl, D.T., Stephens, J.A., Swiler, L.P., & Winokur, J.G., 2020. DAKOTA, A Multilevel Parallel Object-Oriented Framework for Design Optimization, Parameter Estimation, Sensitivity Analysis, and Uncertainty Quantification Acknowledgment. Technical Report SAND2020-12495, Sandia National Laboratory, Albuquerque, NM. URL: https://dakota.sandia.gov/sites/default/files/docs/6.13/Users-6.13.0.pdf.

Algina, J., 2008. Confidence intervals for the squared multiple semipartial correlation coefficient. Journal of Modern Applied Statistical Methods 7, 2–10. https://doi.org/10.22237/jmasm/1209614460.

Aures, A., Bostelmann, F., Hursin, M., Leray, O., 2017. Benchmarking and application of the state-of-the-art uncertainty analysis methods XSUSA and SHARK-X. Annals of Nuclear Energy 101, 262–269. https://doi.org/10.1016/j.anucene.2016.11.025.

Aures, A., Berner, N., Pautz, A., Zwermann, W., 2020. Uncertainty and sensitivity analysis of PWR mini-core transients in the presence of nuclear data uncertainty using non-parametric tolerance limits. Annals of Nuclear Energy 137,. https://doi.org/10.1016/j.anucene.2019.107146 107146.

Bostelmann, F., 2020. Systematic sensitivity and uncertainty analysis of sodium-cooled fast reactor systems. Ph.D. thesis École polytechnique fédérale de Lausanne, Switzerland. URL: https://infoscience.epfl.ch/record/274286.

Bostelmann, F., Weiß, F.-P., Aures, A., Velkov, K., Zwermann, W., Rearden, B.T., Jessee, M.A., Williams, M.L., Wiarda, D., Wieselquist, W.A., 2015a. Uncertainty and Sensitivity Analysis in Criticality Calculations with Perturbation Theory and Sampling. In: MC2015, Nashville, TN, April 19–23.

Bostelmann, F., Zwermann, W., Krzykacz-Hausmann, B., Gallner, L., Aures, A., Velkov, K., 2015b. Sampling-Based Nuclear Data Uncertainty Analysis in Criticality and Depletion Calculations. In: In MC2015 April 19–23. Nashville, TN.

Bostelmann, F., Krzykacz-Hausmann, B., Aures, A., Zwermann, W., Velkov, K., 2018. Sensitivity Indices for Nuclear Data Uncertainty Analysis with XSUSA and TSUNAMI. In: BEPU2018, Real Collegio, Lucca, Italy, May 13–19, pp. 13–19.

Boyack, B., Catton, I., Duffey, R., Griffith, P., Katsma, K., Lellouche, G., Levy, S., Rohatgi, U., Wilson, G., Wulff, W., Zuber, N., 1990. Quantifying reactor safety margins part 1: An overview of the code scaling, applicability, and uncertainty evaluation methodology. Nuclear Engineering and Design 119, 1–15. https://doi.org/10.1016/0029-5493(90)90071-5.

Broadhead, B.L., Rearden, B.T., Hopper, C.M., Wagschal, J.J., Parks, C.V., 2004. Sensitivity- and Uncertainty-Based Criticality Safety Validation Techniques. Nuclear Science and Engineering 146 (3), 340–366. https://doi.org/10.13182/NSE03-2.

Chadwick, M., Herman, M., Obložinský, P., Dunn, M., Danon, Y., Kahler, A., Smith, D., Pritychenko, B., Arbanas, G., Arcilla, R., Brewer, R., Brown, D., Capote, R., Carlson, A., Cho, Y., Derrien, H., Guber, K., Hale, G., Hoblit, S., Holloway, S., Johnson, T., Kawano, T., Kiedrowski, B., Kim, H., Kunieda, S., Larson, N., Leal, L., Lestone, J., Little, R., McCutchan, E., MacFarlane, R., MacInnes, M., Mattoon, C., McKnight, R., Mughabghab, S., Nobre, G., Palmiotti, G., Palumbo, A., Pigni, M., Pronyaev, V.G., Sayer, R., Sonzogni, A., Summers, N., Talou, P., Thompson, I., Trkov, A., Vogt, R., Van Der Marck, S., Wallner, A., White, M., Wiarda, D., Young, P., 2011. ENDF/B-VII.1 Nuclear Data for Science and Technology: Cross Sections, Covariances, Fission Product Yields and Decay Data. Nuclear Data Sheets 112, 2887–2996. https://doi.org/10.1016/j.nds.2011.11.002.

Cohen, J., 2003. Applied Multiple Regression/Correlation Analysis for the Behavioral Sciences. Lawrence Erlbaum Associates, London.

D'Auria, F., Camargo, C., Mazzantini, O., 2012. The Best Estimate Plus Uncertainty (BEPU) approach in licensing of current nuclear reactors. Nuclear Engineering and Design 248, 317–328. https://doi.org/10.1016/j.nucengdes.2012.04.002.

Glaeser, H., 2008. Methodenentwicklung und exemplarische Anwendungen zur Bestimmung der Aussagesicherheit von Rechenprogrammergebnissen. Technical Report GRS-A-3443. Gesellschaft für Anlagen- und Reaktorsicherheit, Garching, Germany https://www.grs.de/publikation/grs-A-3443.

Glaeser, H., 2012. Thermohydraulische Rechenmethoden zu Transienten und Störfällen im Reaktorkühlkreislauf unter besonderer Berücksichtigung mehrdimensionaler Strömungen (ATHLET, FLUBOX, CFX). Technical Report GRS-A-3644, Gesellschaft für Anlagen- und Reaktorsicherheit, Garching, Germany. URL: https://www.grs.de/publikation/grs-A-3644.

Golberg, M.A., Cho, H.A., 2004. Introduction to Regression Analysis. WIT Press, Southampton, Boston.

Hursin, M., Scriven, M., Perret, G., Pautz, A., 2016. Uncertainty quantification and representativity analysis of LWR-PROTEUS Phase III experiments using SHARKX. Annals of Nuclear Energy 91, 48–58. https://doi.org/10.1016/j.anucene.2015.12.035.

Ilas, G., Liljenfeldt, H., 2017. Decay heat uncertainty for BWR used fuel due to modeling and nuclear data uncertainties. Nuclear Engineering and Design 319, 176–184. https://doi.org/10.1016/j.nucengdes.2017.05.009.

Krzykacz-Hausmann, B., 2006. An approximate sensitivity analysis of results from complex computer models in the presence of epistemic and aleatory uncertainties. Reliability Engineering and System Safety 91, 1210–1218. https://doi.org/10.1016/j.ress.2005.11.019.

Little, R., Kawano, T., Hale, G., Pigni, M., Herman, M., Obložinský, P., Williams, M., Dunn, M., Arbanas, G., Wiarda, D., McKnight, R., McKamy, J., Felty, J., 2008. Low-fidelity Covariance Project. Nuclear Data Sheets 109, 2828–2833. https://doi.org/10.1016/j.nds.2008.11.018.

Martinez, J.S., Zwermann, W., Gallner, L., Puente-Espel, F., Cabellos, O., Velkov, K., Hannstein, V., 2014. Propagation of neutron cross section, fission yield, and decay data uncertainties in depletion calculations. Nuclear Data Sheets. https://doi.org/10.1016/j.nds.2014.04.112.

Müller, P., 1980. Wahrscheinlichkeitsrechnung und Mathematische Statistik, Lexikon der Statistik. Akademie-Verlag, Berlin.

Olkin, I., Finn, J.D., 1995. Correlation Redux. Psychological Bulletin 118, 155–164.

Rearden, B.T., Williams, M.L., Jessee, M.A., Mueller, D.E., Wiarda, D.A., 2011. Sensitivity and uncertainty analysis capabilities and data in SCALE. Nuclear Technology 174, 236–288. https://doi.org/10.13182/NT174-236.

Rochman, D., Koning, A.J., Da Cruz, D.F., 2011. Uncertainties for the Kalimer Sodium Fast Reactor: Void Reactivity Coefficient, k eff, β eff, Depletion and Radiotoxicity. Journal of Nuclear Science and Technology 48, 1193–1205. doi: 10.1080/18811248.2011.9711807.

Rochman, D., Zwermann, W., van der Marck, S.C., Koning, A.J., Sjöstrand, H., Helgesson, P., Krzykacz-Hausmann, B., 2014. Efficient Use of Monte Carlo: Uncertainty Propagation. Nuclear Science and Engineering 177, 337–349. https://doi.org/10.13182/NSE13-32.

Rochman, D., Leray, O., Hursin, M., Ferroukhi, H., Vasiliev, A., Aures, A., Bostelmann, F., Zwermann, W., Cabellos, O., Diez, C., Dyrda, J., Garcia-Herranz, N., Castro, E., van der Marck, S., Sjöstrand, H., Hernandez, A., Fleming, M., Sublet, J.-C., Fiorito, L., 2017. Nuclear Data Uncertainties for Typical LWR Fuel Assemblies and a Simple Reactor Core. Nuclear Data Sheets 139, 1–76. https://doi.org/10.1016/j.nds.2017.01.001.

Saltelli, A., Ratto, M., Andres, T., Campolongo, F., Cariboni, J., Gatelli, D., Saisana, M., Tarantola, S., 2008. Global Sensitivity Analysis: The Primer. John Wiley & Sons, Ltd.. https://doi.org/10.1002/9780470725184.

Saltelli, A., Annoni, P., Azzini, I., Campolongo, F., Ratto, M., Tarantola, S., 2010. Variance based sensitivity analysis of model output. Design and estimator for the total sensitivity index. Computer Physics Communications 181, 259–270. https://doi.org/10.1016/j.cpc.2009.09.018.

Salvatores, M., Jacqmin, R., 2008. Uncertainty and Target Accuracy Assessment for Innovative Systems Using Recent Covariance Data Evaluations. Technical Report NEA/WPEC-26. OECD/NEA https://oecd-nea.org/download/wpec/volume26/volume26.pdf.

Shibata, K., Iwamoto, O., Nakagawa, T., Iwamoto, N., Ichihara, A., Kunieda, S., Chiba, S., Furutaka, K., Otuka, N., Ohsawa, T., Murata, T., Matsunobu, H., Zukeran, A., Kamada, S., Katakura, J.-I., 2012. JENDL-4.0: A New Library for Nuclear Science and Engineering. Journal of Nuclear Science and Technology 48, 1–30. https://doi.org/10.1080/18811248.2011.9711675.

Sobol, I.M. (1993). Sensitivity analysis for non-linear mathematical models. Mathematical Modelling and Computational Experiment, 1, 407–414. https://doi.org/1061-7590/93/04407-008.

Sturek, F., Agrenius, L., Osifo, O., 2006. Measurements of decay heat in spent nuclear fuel at the Swedish interim storage facility, Clab. Technical Report R-05-62. Svensk Kärnbränslehantering AB, Stockholm, Sweden https://www.skb.com/publication/1472024.

Swiler, L.P., Adams, B.M., Wieselquist, W., 2018. Sample Generation for Nuclear Data. Technical Report SAND2018-10554 Sandia National Laboratories, Albuquerque, NM. URL: https://www.osti.gov/servlets/purl/1474254.

Wieselquist, W., Zhu, T., Vasiliev, A., Ferroukhi, H., 2013. PSI Methodologies for Nuclear Data Uncertainty Propagation with CASMO-5M and MCNPX: Results for OECD/NEA UAM Benchmark Phase I. Science and Technology of Nuclear Installations 2013, 1–15. https://doi.org/10.1155/2013/549793.

Wieselquist, W.A., Lefebvre, R.A., Jessee, M.A., 2020. SCALE Code System, Version 6.2.4. Technical Report ORNL/TM-2005/39, Oak Ridge National Laboratory, Oak Ridge, TN. URL: https://www.ornl.gov/file/scale-62-manual/display.

Williams, M.L., 1986. Perturbation Theory for Nuclear Reactor Analysis. In: Ronen, Y. (Ed.), Handbook of Nuclear Reactors Calculations, vol. III. CRC Press, pp. 63–188.

Williams, M.L., Broadhead, B.L., Parks, C.V., 2001. Eigenvalue Sensitivity Theory for Resonance-Shielded Cross Sections. Nuclear Science and Engineering 138, 177–191. https://doi.org/10.13182/NSE00-56.

Williams, M. L., Ilas, G., Jessee, M. a., Rearden, B. T., Wiarda, D., Zwermann,W., Gallner, L., Klein, M., Krzykacz-Hausmann, B., & Pautz, A. (2013). Astatistical sampling method for uncertainty analysis with SCALE and XSUSA.1035Nuclear Technology,183, 515–526. https://doi.org/10.13182/NT12-112.

Zhu, T., Vasiliev, A., Ferroukhi, H., Pautz, A., 2015. NUSS: A tool for propagating multigroup nuclear data covariances in pointwise ACE-formatted nuclear data using stochastic sampling method. Annals of Nuclear Energy 75, 713–722. https://doi.org/10.1016/j.anucene.2014.09.013.

Zhu, T., Vasiliev, A., Ferroukhi, H., Rochman, D., Pautz, A., 2016. Testing the sampling-based NUSS-RF tool for the nuclear data-related global sensitivity analysis with Monte Carlo neutronics calculations. Nuclear Science and Engineering 184, 69–83. https://doi.org/10.13182/NSE14-142.